

An Accurate Computation of Highly Oscillatory Integrals with Critical Points

Sakhi Zaman
Department of Basic Sciences,
University of Engineering and Technology Peshawar, Pakistan,
Email: sakhizaman75@gmail.com

Suliman
Department of Basic Sciences,
University of Engineering and Technology Peshawar, Pakistan,
Email: salman1985.geyes@gmail.com

Siraj-ul-Islam
Department of Basic Sciences,
University of Engineering and Technology Peshawar, Pakistan,
Email: siraj.islam@gmail.com

Received: 14 July, 2017 / Accepted: 31 January, 2018 / Published online: 31 August, 2018

Abstract. New methods are proposed for evaluation of one-dimensional highly oscillatory integrals with and without critical points. These integrals are hard to approximate due to the existence of high oscillations of the integrand and to take care of the critical point in the domain interval. Levin procedure with Gaussian radial basis function is implemented to evaluate oscillatory integrals without critical point. The meshless method is coupled with multi-resolution analysis in a new shape to handle the critical points. Test problems verify accuracy and efficiency of the new methods.

AMS (MOS) Subject Classification Codes: 35S29; 40S70; 25U09

Key Words: Gaussian radial basis function, Oscillatory integrals with critical point(s), Splitting procedure, Multi-resolution quadratures.

1. INTRODUCTION

Highly oscillatory integrals (HOIs) have many practical applications in physical sciences, particularly in the field of optics, quantum mechanics, acoustics and electromagnetics [26, 16]. The general form of these integrals is given as

$$I[f] = \int_a^b f(x)e^{i\omega g(x)} dx, \quad (1. 1)$$

where the functions $f, g : [a, b] \rightarrow \mathbb{R}$ are non-oscillatory smooth functions, $\omega \gg 1$ and $g(x)$ may or may not have critical points in $[a, b]$. The parameter ω represents frequency of the oscillations. Large value of ω implies that the integrand is highly oscillatory. Many quadrature rules such as Simpson rule and Gauss-Legendre quadrature etc. fail to compute integrals of the form (1.1) for large ω .

In the last two decades, many state of the art methods have been developed for computation of one-dimensional HOIs, which include asymptotic method [14, 27, 24, 30], numerical steepest decent method [13, 2, 10, 1], Filon(-type) method [7, 8, 25, 12, 11], Levin(-type) method [23, 19, 20, 17, 21, 31] and generalized quadrature rule [29, 5].

The asymptotic expansion theory which is considered by Filon [8] is one of the best method for evaluation of HOIs. This method has been modified in many forms like [24]. The method [24] gives a high asymptotic order when the frequency $\omega \rightarrow \infty$, but the limitations of this method is that it can solve HOIs with linear phase functions only [13, 6].

Few methods have been used which are applicable to approximate oscillatory integrals with stationary points [24, 9, 28, 27, 4]. In [24], the authors have used Gauss-type quadrature rules with complex-valued nodes and weights to approximate oscillatory integrals with stationary points of high order. The method is based on substituting the original interval of integration by a set of contours in the complex plane, corresponding to the paths of steepest descent. A high asymptotic order of convergence is attained for this type of integrals.

Superinterpolation method is used [9] in which the values of the integrand at certain complex points close to the critical points, can actually yield a higher asymptotic order approximation to the integral. The asymptotic convergence rates of Filon-type methods can be doubled at no additional cost. The asymptotic order of convergence by the superinterpolation method reaches to $O(\omega^{-2s-1})$.

Levin method [23] has got much attention as it can compute HOIs with complicated phase functions. In this method, a one-dimensional HOI is converted into an ordinary differential equation and then, ultimately, the equation is solved by the collocation method. Levin [23] has used monomials basis function. In the proposed work, Gaussian radial basis function is used in the Levin's approach.

The Levin collocation procedure fails to approximate HOIs with critical point as in case of critical point $g'(x_0) = 0$, where $x_0 \in [a, b]$ is unique critical point of $g(x)$. The Levin ODE can not be solved for the unknown parameters of the collocation method reported in [23]. The author [28] has introduced a splitting algorithm, which based on unified approach of the Levin collocation method and the two points Gaussian quadrature rule to evaluate HOIs with critical point.

Recently, Siraj-ul-Islam et.al. [20] proposed a new algorithm, following the procedure [28], in which a meshless collocation method with multiquadric RBF is couple with hybrid function based quadrature and attained a high convergence rate. In this work, the authors have proved some theoretically error bounds of the component methods of the new algorithm.

The current work is the modified form of [20] in which a meshless collocation method based on Gaussian RBF is coupled with the multi-resolution quadrature rules. Multi-resolution quadrature rules based on hybrid functions or Haar wavelets is used to tackle the critical point(s). In this procedure, the domain interval is split into two or more sub-intervals in order to isolate the critical point. The integral over a small interval having

TABLE 1. **Nomenclature Box:**

Symbols	Discription
RBF	Radial basis functions
GRBF	Gaussian radial basis functions
HOIs	Highly oscillatory integrals
$Q_G^{MM}[f]$	Meshless procedure with Gaussian RBF
$Q_{HF}[f]$	Quadrature based on hybrid functions
$Q_{HW}[f]$	Quadrature based on Haar wavelets
$Q_\xi[f]$	Splitting procedure based on hybrid functions and meshless method
$Q_\eta[f]$	Splitting procedure based on Haar wavelets and meshless method
ϵ	Shape parameter of the Gaussian radial basis functions
ω	Frequency parameter
ξ	Splitting parameter
κ	Order of the critical point

critical point is evaluated by the multi-resolution quadratures and the remaining integrals are approximated by the meshless collocation procedure. Some benchmark test problems are included to verify accuracy of the proposed algorithm.

The rest of paper is organized as follows:

In Section 2, some quadrature rules like meshless collocation procedure and multi-resolution quadratures based on hybrid functions and Haar wavelets are discussed. In Section 3, the proposed splitting algorithm and error bounds of the component methods are discussed. In Section 4, numerical results are reported and in Section 5, brief conclusions of the work are included.

2. QUADRATURE RULES

Some quadrature rules are discussed in this section.

2.1. Meshless collocation procedure. To compute highly oscillatory integrals of the form (1. 1) with no critical point by Levin's procedure, we find an approximate function $\tilde{S}(x)$ that satisfies the ODE:

$$S'(x) + i\omega g'(x)S(x) = f(x). \quad (2. 2)$$

Substituting (2. 2) into (1. 1), we get

$$\begin{aligned} I[f] &= \int_a^b [\tilde{S}'(x) + i\omega g'(x)\tilde{S}(x)]e^{i\omega g(x)} dx \\ &= \int_a^b d[\tilde{S}(x)e^{i\omega g(x)}] \\ &= \tilde{S}(b)e^{i\omega g(b)} - \tilde{S}(a)e^{i\omega g(a)}. \end{aligned} \quad (2. 3)$$

In this procedure, we assume that $\tilde{S}(x) = \sum_{k=1}^m \delta_k \varphi_k(x, \epsilon)$ be an approximate solution of the ODE (2. 2). The unknown coefficients δ_k , $k = 1, 2, \dots, m$ can be determined by the

following interpolation condition

$$\tilde{S}'(x_j) + i\omega g'(x_j)\tilde{S}(x_j) = f(x_j), \quad j = 1, 2, \dots, m. \quad (2.4)$$

Equation (2.4) gives a system of m -linear equations in m -unknowns and can be written in matrix notation as

$$\mathbf{A}\delta = \mathbf{f},$$

where

$$\delta = [\delta_1, \delta_2, \dots, \delta_m]^\top, \quad \mathbf{f} = [f_1, f_2, \dots, f_m]^\top,$$

and \mathbf{A} is an $m \times m$ square matrix with entries:

$$a_{jk} = \varphi'_{jk}(r, \epsilon) + i\omega g(x_k)\varphi_{jk}(r, \epsilon), \quad j, k = 1, 2, \dots, m.$$

To find the values of δ , system of linear equations (2.4) can be solved by LU-factorization or Gauss-elimination method and consequently, one can find the approximate solution $\tilde{S}(x)$.

In the proposed work, a Gaussian RBF $\varphi(r, \epsilon)$ is used as a basis function, which is defined as

$$\varphi(r, \epsilon) = e^{-\frac{r^2}{\epsilon^2}}, \quad r = |x - x^c|,$$

where x^c are m -centers of the RBF interpolation and ϵ is the shape parameter. The derivative of $\varphi(r, \epsilon)$ is given by

$$\varphi'(r, \epsilon) = \frac{-2r}{\epsilon^2} e^{-\frac{r^2}{\epsilon^2}}.$$

The approximate solution by the meshless procedure given in (2.3) is denoted by $Q_G^{MM}[f]$, which depends on selecting an optimal value of the shape parameter ϵ . An algorithm [17] is used in the current work for finding ϵ .

2.2. Hybrid and Haar functions. In this section, some formulae for multi-resolution quadratures are discussed. The detail description and derivations of the formulae for multi-resolution quadratures based on hybrid functions $Q_{HF}[f]$ and Haar wavelets $Q_{HW}[f]$ are discussed in [18, 3].

Formula of $Q_{HF}[f]$ of order 8 for evaluating integrals of the form $I[f] = \int_a^b f(x) dx$ is given by

$$\begin{aligned} Q_{HF}[f] = & \frac{8h}{1935360} \sum_{k=1}^n \left[295627 f\left(a + \frac{h}{2}(16k-15)\right) + 71329 f\left(a + \frac{h}{2}(16k-13)\right) \right. \\ & + 471771 f\left(a + \frac{h}{2}(16k-11)\right) + 128953 f\left(a + \frac{h}{2}(16k-9)\right) \\ & + 128953 f\left(a + \frac{h}{2}(16k-7)\right) + 471771 f\left(a + \frac{h}{2}(16k-5)\right) \\ & \left. + 71329 f\left(a + \frac{h}{2}(16k-3)\right) + 295627 f\left(a + \frac{h}{2}(16k-1)\right) \right]. \quad (2.5) \end{aligned}$$

The truncation error of $Q_{HF}[f]$ for $a = 0, b = 1$ and $N = 4$, is given by

$$|E| = \frac{3194621 \times h^9}{14515200} f^{(8)}(\varsigma),$$

where $\varsigma \in (a, b)$.

Also, formula of $Q_{HW}[f]$ for computing integral of the form $I[f] = \int_a^b f(x) dx$ is given as

$$Q_{HW}[f] = \frac{b-a}{2M} \sum_{i=1}^N f\left(a + \frac{b-a}{2M}(i-0.5)\right), \quad (2.6)$$

where $N = 2M$.

Truncation error of the quadrature rule $Q_{HW}[f]$ is given by

$$|E| = \frac{h^3}{6} f''(\eta),$$

for some $\eta \in (a, b)$.

3. SPLITTING ALGORITHM AND ERROR BOUNDS

As discussed earlier that the meshless collocation method $Q_G^{MM}[f]$ fails to evaluate highly oscillatory integrals with critical point. An interval splitting procedure is proposed for evaluation of HOIs with critical points.

3.1. Splitting algorithm. According to this procedure, the domain is subdivided in order to isolate the critical point. For this purpose, we define a splitting parameter ξ in terms of frequency ω as

$$\xi = \left(\frac{N}{10\omega}\right)^{\frac{1}{\kappa}}, \quad (3.7)$$

where $a < \xi < b$, $\xi \rightarrow 0$ as $\omega \rightarrow \infty$, for fixed N , and κ is the order of critical point. If $x = a$ is a unique critical point that lies at the lower end of the domain interval i.e. $g'(a) = 0$, then integral (1. 1) can be written in split form as

$$\begin{aligned} I[f] &= \int_a^{a+\xi} f(x) e^{i\omega g(x)} dx + \int_{a+\xi}^b f(x) e^{i\omega g(x)} dx \\ &= I_c[f] + I_{nc}[f]. \end{aligned}$$

The integral $I_c[f]$ contains the critical point and is approximated by $Q_{HF}[f]$ or $Q_{HW}[f]$ with N quadrature points and $I_{nc}[f]$ having no critical point is computed by $Q_G^{MM}[f]$ for m equal subintervals. The resulting value of (1. 1) is given as

- i. If $I_c[f]$ is evaluated by the hybrid function of order 8, then compute

$$Q_\xi[f] = Q_{HF}[f] + Q_G^{MM}[f].$$

- ii. If Haar wavelets based quadrature is used for $I_c[f]$, then compute

$$Q_\eta[f] = Q_{HW}[f] + Q_G^{MM}[f].$$

- iii. When the critical point $x = x_0 \in [a, b]$ lies in the middle of the integration domain, then integral (1. 1) can be split at $x = \xi$ as

$$\begin{aligned} I[f] &= \int_a^{x_0-\xi} f(x) e^{i\omega g(x)} dx + \int_{x_0-\xi}^{x_0+\xi} f(x) e^{i\omega g(x)} dx + \int_{x_0+\xi}^b f(x) e^{i\omega g(x)} dx \\ &= I_1[f] + I_2[f] + I_3[f], \end{aligned}$$

where ξ is the splitting parameter satisfying (3.7). The integral $I_2[f]$ contains the critical point $x_0 \in [x_0 - \xi, x_0 + \xi]$ and is approximated by the $Q_{HF}[f]$. The remaining integrals are computed by the meshless procedure $Q_G^{MM}[f]$.

3.2. Error bounds. Some error bounds of the individual methods in terms of ω are obtained to ensure the asymptotic convergence rate of the new algorithm.

Lemma 3.3. *Suppose that the oscillator g has a critical point at $x = a$ of order $(\kappa - 1)$. Let ξ satisfy $10 M_\xi \omega = N$ for large ω , where $M_\xi = \max_{x \in [a, \xi]} |g(x) - g(a)|$. Then the error bound for computing $I_c[f]$ by the $Q_{HF}[f]$ for N quadrature points, is given by*

$$E_c = |I_c[f] - Q_{HF}[f]| \leq \frac{C(\xi - a)}{4.54 \times 10^8} = \frac{C((\frac{N}{10\omega})^{1/\kappa} - a)}{4.54 \times 10^8}, \quad \omega \gg 1,$$

where the constant C is independent of ξ and ω .

Proof. See [20]. □

Lemma 3.4. *Suppose that the function $g(x)$ has a critical point at $x = a$ of order $(\kappa - 1)$. For $\xi = (\frac{N}{10\omega})^{1/\kappa}$ and $\delta = \min_{x \in [\xi, b]} |g'(x)|$, the error bound of the meshless procedure for computing I_{nc} , is given by*

(1) For $\xi < x_1 < x_2 < \dots < x_m = b$, we have

$$E_{nc} = |I_{nc}[f] - Q_G^{MM}[f]| = O\left(\frac{(b - \xi)^m}{(\omega)^{1/\kappa}}\right), \quad \omega \gg 1.$$

(2) For $a < x_1 < x_2 < \dots < x_m = b$, i.e. the end points of the interval are included, then

$$E_{nc} = |I_{nc}[f] - Q_G^{MM}[f]| = O\left(\frac{(b - x_1)^{m-1}}{\omega^2}\right), \quad \omega \gg 1.$$

Proof. See [20]. □

According to the splitting procedure, integral (1.1) can be written in split form as

$$I[f] = I_c[f] + I_{nc}[f].$$

Integral $I_c[f]$ is computed by the hybrid function and $I_{nc}[f]$ is computed by the meshless procedure. The resulting value of the integral is given by

$$Q_\xi[f] = Q_{HF}[f] + Q_G^{MM}[f].$$

The error bound of the splitting method $Q_\xi[f]$ depends upon the two methods $Q_{HF}[f]$ and $Q_G^{MM}[f]$.

Combining the results of Theorems 1 and 2, the error bound of the splitting procedure $Q_\xi[f]$ is given as

$$|Error| = |I[f] - Q_\xi[f]| \leq \min\left(\frac{C((\frac{N_0}{10\omega})^{1/\kappa} - a)}{4.54 \times 10^8}, \frac{(b - x_1)^{m-1}}{\omega^2}\right). \quad (3.8)$$

TABLE 2. L_{abs} produced by $Q_G^{MM}[f]$, $\epsilon \in [0, 0.5]$ for test problem 4.1.

ω	$m = 10$	$m = 20$	$m = 30$
10^5	$6.6078e - 09$	$4.4537e - 10$	$2.2092e - 10$
10^6	$2.1118e - 11$	$1.4378e - 10$	$4.0540e - 09$
10^7	$6.2537e - 13$	$5.0288e - 10$	$1.9846e - 10$
10^8	$5.9605e - 14$	$7.8408e - 11$	$4.0268e - 12$
10^9	$1.1187e - 15$	$1.2355e - 12$	$4.7708e - 13$
10^{10}	$2.6504e - 16$	$8.0227e - 14$	$5.4330e - 14$

Equation (3. 8) shows that the method $Q_\xi[f]$ attains asymptotic order of convergence $O(\omega^{-2})$.

4. NUMERICAL EXAMPLES AND DISCUSSION

In this section, the proposed methods are tested on some benchmark test problems reported in [25, 28, 27, 22]. The reference solution is obtained by MAPLE 15. The absolute errors L_{abs} , relative errors L_{re} and absolute scaled errors are computed in each test problem. Results of the new methods are compared with the results of the methods [25, 28, 27, 22]. Computation is performed by using MATLAB platform.

Example 4.1. Consider the computation of integral [25]:

$$I_1[f] = \int_0^1 e^{10x} e^{i\omega(x^2+x)} dx. \quad (4. 9)$$

The integral is highly oscillatory and is evaluated by the new methods $Q_G^{MM}[f]$, $Q_{HW}[f]$ and $Q_{HF}[f]$. Results in terms of absolute errors are shown in figures 1-2 and table 2. In figure 1, the absolute errors scaled by ω^3 of $Q_G^{MM}[f]$ and its comparison with the results of [25] is shown. From figure 1, it is clear that the performance of the method $Q_G^{MM}[f]$ is better than the method [25]. The meshless procedure $Q_G^{MM}[f]$ is tested for higher frequencies and nodes. The results are shown in table 2. It is clear from the table that as we increase the value of ω or nodal points, accuracy of the method is improving.

Integral (4. 9) is evaluated by the proposed methods $Q_G^{MM}[f]$, $Q_{HW}[f]$ and $Q_{HF}[f]$ for varying frequency and fixed nodes. The absolute errors are shown in figure 2 (left), while in figure 2 (right), fixed the frequency and varying nodal points. It is shown in the figures that the method $Q_G^{MM}[f]$ gives better accuracy than all the other methods. The main advantage of the new method $Q_G^{MM}[f]$ is that it improves the accuracy on increasing values of the ω for small nodal points.

Example 4.2. Consider the numerical evaluation of integral [27]:

$$I_2[f] = \int_0^1 \cos x e^{i\omega(x^2+x)} dx. \quad (4. 10)$$

The integral (4. 10) is highly oscillatory and the oscillations of the integrand are shown in figure 9 (left). The integral is computed by the proposed methods $Q_G^{MM}[f]$, $Q_{HF}[f]$ and $Q_{HW}[f]$. Absolute errors are shown in figures 3-4. The absolute errors scaled by ω^4

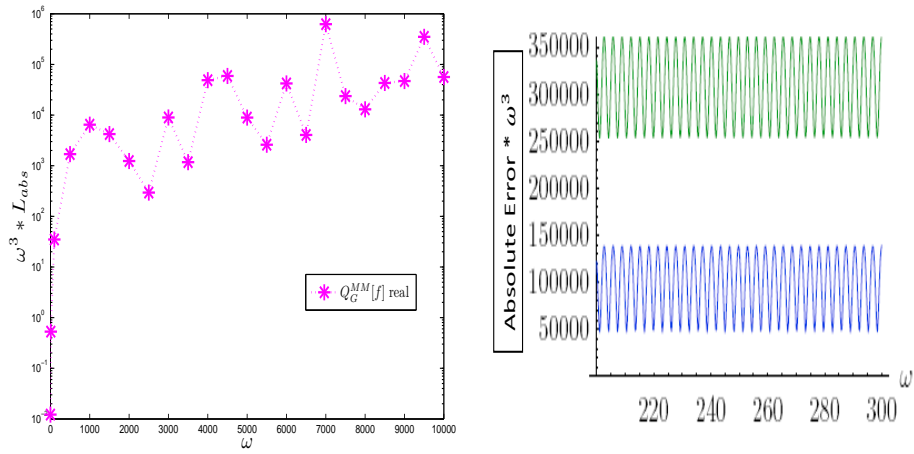


FIGURE 1. (left) L_{abs} scaled by ω^3 of $Q_G^{MM}[f]$ for $m = 30$, (right) L_{abs} scaled by ω^3 of the Filon method (top) and Levin method [25] for test problem 4.1.

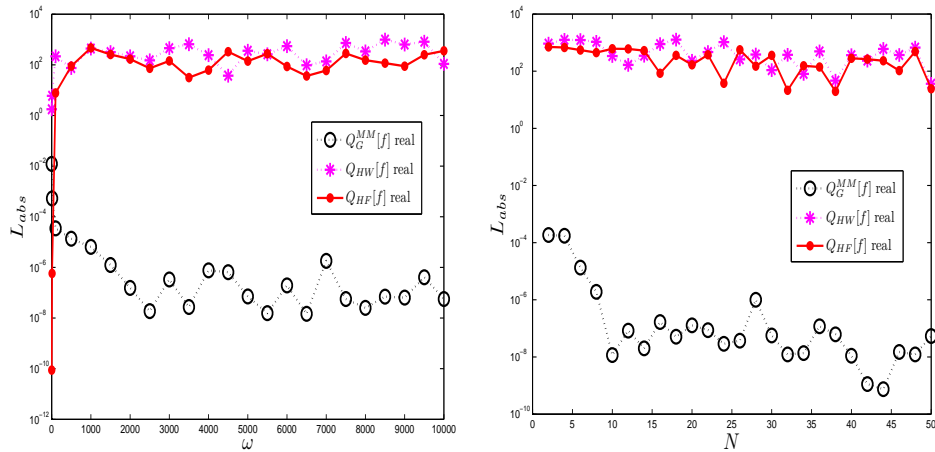


FIGURE 2. (left) L_{abs} of the proposed methods for $m = 30$, (right) L_{abs} of the proposed methods, $\omega = 10^4$ for test problem 4.1.

of $Q_G^{MM}[f]$ are calculated and are shown in figure 3. Comparison of the proposed methods with the results of method reported in [27] is performed. From figure 3, it is clear that the proposed method $Q_G^{MM}[f]$ is more accurate than all the other methods.

Integral (4. 10) is evaluated by the proposed methods $Q_G^{MM}[f]$, $Q_{HW}[f]$ and $Q_{HF}[f]$ for varying frequency and fixed nodes . The results are given in figure 4 (left). In figure 4 (right), the frequency is fixed and nodal points are variable. It is clear from figures 3 and 4 that the new method $Q_G^{MM}[f]$ is accurate than all the other methods. The main advantage

of the new method $Q_G^{MM}[f]$ is that it improve the accuracy on increasing the value of ω for small nodal points. From figure 3 (left), it is confirmed that the new method $Q_G^{MM}[f]$ attains an asymptotic order of convergence $O(\omega^{-4})$.

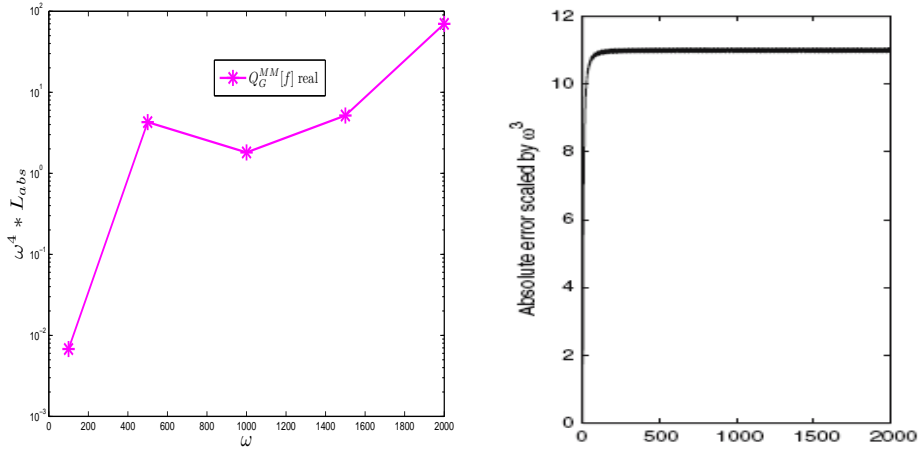


FIGURE 3. (left) L_{abs} scaled by ω^4 of $Q_G^{MM}[f]$ for $m = 30$, (right) L_{abs} scaled by ω^3 of the method reported in [27] for test problem 4.2.

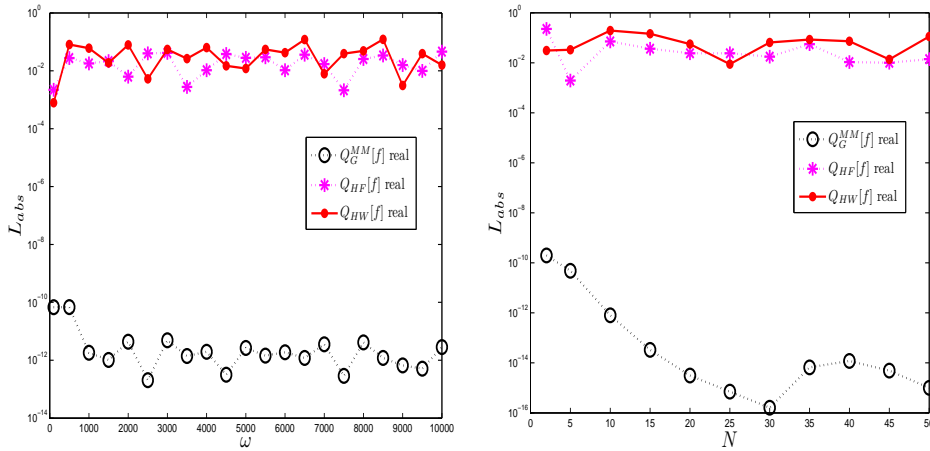


FIGURE 4. (left) L_{abs} of the proposed methods, $m = 30$,(right) L_{abs} of the proposed methods, $\omega = 10^5$ for test problem 4.2.

Example 4.3. Consider the following integral [28]:

$$I_3[f] = \int_0^1 e^{i\omega x^2} dx. \tag{4.11}$$

The integral (4.11) has a critical point at $a = 0$. Irregular oscillations of the integrand are shown in figure 6 (right). Integral (4.11) is approximated by the proposed splitting algorithm. Results are shown in figures 5-6. The results obtained by the new splitting method for fixed nodal points are shown in figure 5 (left), while comparison of the method reported in [28] is shown in figure 5 (right). From the figure, it is clear that the proposed procedure is relatively better than the method reported in [28].

The integral is evaluated by $Q_G^{MM}[f]$ for larger values of ω . Results in terms of scaled absolute errors are shown in figure 6 (left). From the figure it is clear that the new method attains asymptotic convergence $O(\omega^{-3})$.

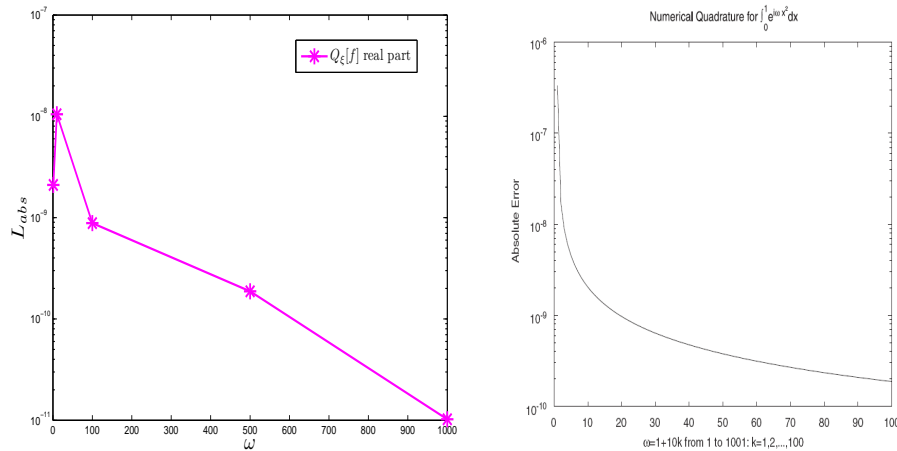


FIGURE 5. (left) L_{abs} produced by $Q_\xi[f]$ for $m = 30$, (right) L_{abs} of method reported in [28] for test problem 4.3.

Example 4.4. Consider the following integral [22]:

$$I_4[f] = \int_{-1}^1 (x^2 + x) e^{i\omega \sqrt{1+(x+1)^2}} dx \quad (4.12)$$

The integrand has a critical point at the lower end point $x = -1$. Irregular oscillations of the integrand is shown in figure 9 (right). The integral is approximated by the new splitting procedure $Q_\xi[f]$. Results in the form of relative errors are shown in figures 7-8. Accuracy obtained by the new splitting method for fixed frequency is shown in figure 7 (left), while comparison with the method [22] is shown in figure 7 (right). In figure 7, it is shown that the relative errors of $Q_\xi[f]$ are decreased up to $O(10^{-9})$, while in [22] it is decreased up to $O(10^{-6})$. The results obtained by the new splitting method for varying frequency and fixed nodes, are shown in figure 8 (left), while the results for varying nodal points and fixed frequency are given in figure 8 (right). It is obvious from the figure that the proposed splitting algorithm performs better than the methods reported in the cited literature.

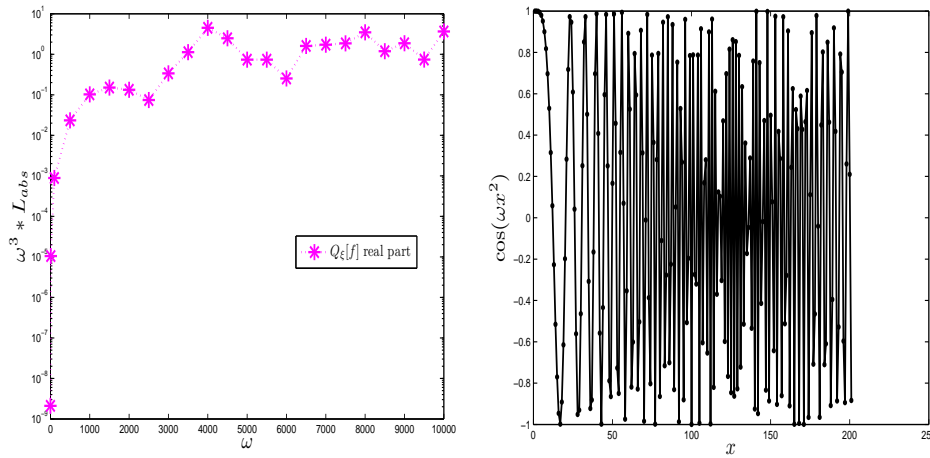


FIGURE 6. Test problem 4.3, (left) L_{abs} scaled by ω^3 for $m = 30$, (right) the oscillatory behavior of the integrand of $I_3[f]$ for $\omega = 500$.

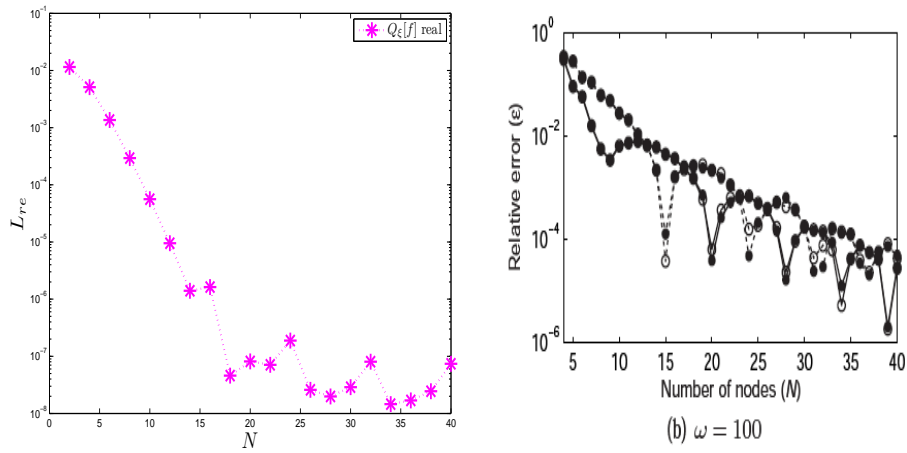


FIGURE 7. (left) L_{re} produced by $Q_\xi[f]$ for $\omega = 100$, (right) L_{re} of method reported in [22] for test problem 4.4.

Example 4.5. Consider the computation of integral [15]:

$$I_5[f] = \int_0^1 \frac{e^{i\omega x}}{1+x} dx. \tag{4.13}$$

The integral is highly oscillatory and is evaluated by the new method $Q_G^{MM}[f]$. Absolute errors scaled by ω^3 are computed and are shown in figure 10 (left). The results of the new methods are compared with the results of Filon method [15]. It is shown in the figure that our method gives $O(10^{-4})$, while the Filon method gives $O(1.8 \times 10^0)$ for the same

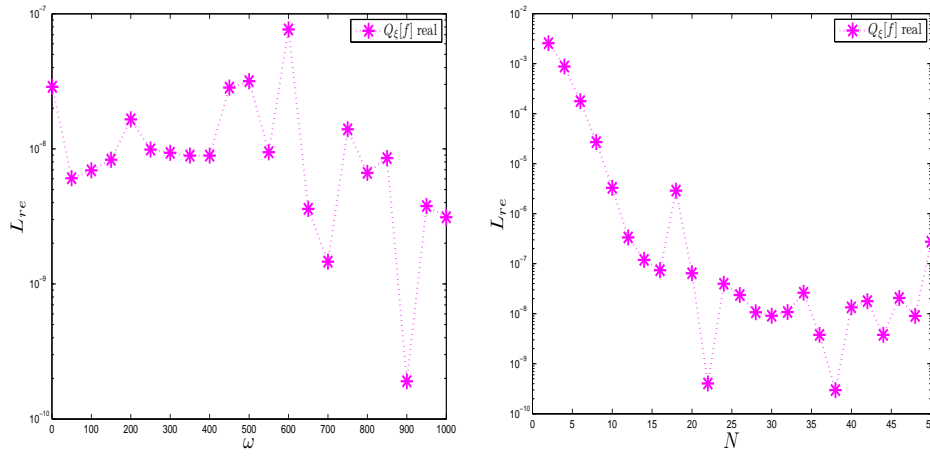


FIGURE 8. (left) L_{re} produced by $Q_{\xi}[f]$ for $m = 30$, (right) L_{re} produced by $Q_{\xi}[f]$, $\omega = 1000$ for test problem 4.4.

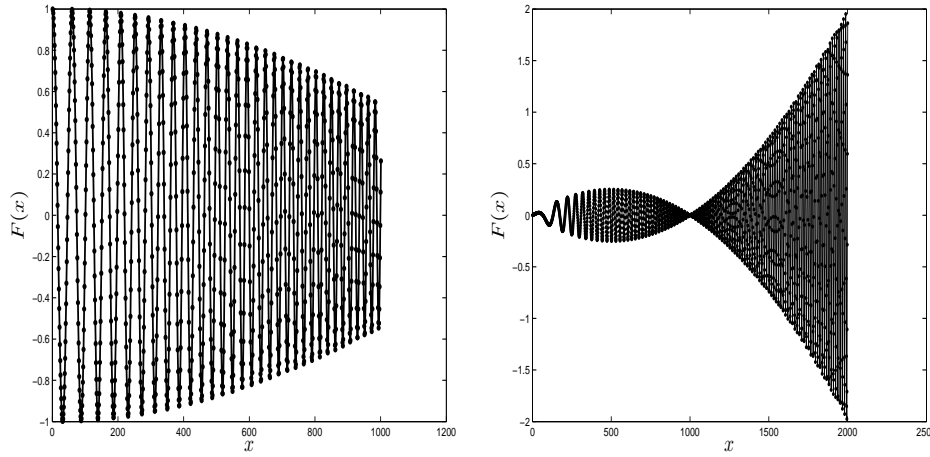


FIGURE 9. Oscillatory behavior of the integrand of (left) $I_2[f]$ for $\omega = 100$ (right) $I_4[f]$ for $\omega = 500$.

frequency. This shows that the results of the proposed method are more accurate than the method reported in [15].

5. CONCLUSION

In this paper, three methods $Q_G^{MM}[f]$, $Q_{HF}[f]$ and $Q_{HW}[f]$ are applied to approximate HOIs without critical point(s). It has been shown that the method $Q_G^{MM}[f]$ gives better accuracy than all the other quadrature rules. Secondly, the new splitting technique $Q_{\xi}[f]$ is

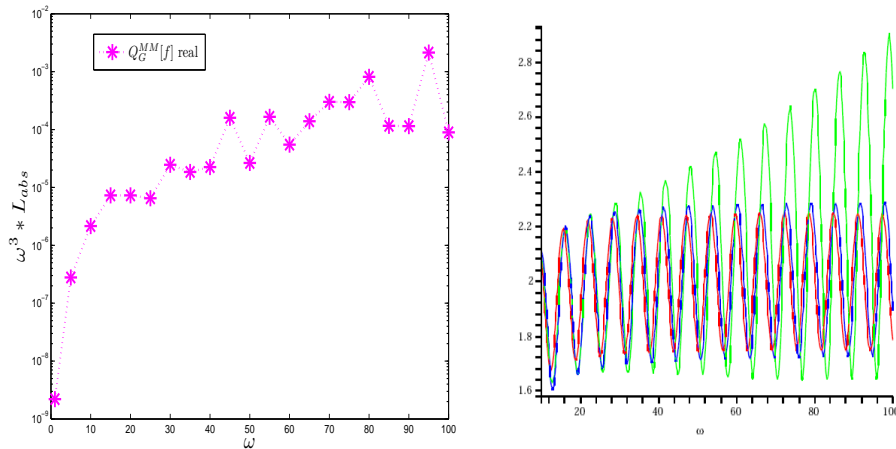


FIGURE 10. (left) L_{abs} scaled by ω^3 of $Q_G^{MM}[f]$ for $m = 30$, (right) L_{abs} scaled by ω^3 of the method in [15] for test problem 4.5.

X

applied for numerical evaluation of HOIs with critical point(s), which unifies the $Q_G^{MM}[f]$ and multi-resolution analysis. This technique attains high asymptotic order of convergence. Numerical examples verified better performance of the proposed methods. The technique is extended to integrable singular integrals like Cauchy principal value integrals with oscillatory kernels. The work is under review.

6. ACKNOWLEDGMENTS

I would like to thank my supervisor, Prof. Siraj-ul-Islam, for the patient guidance and encouragement, he has provided us for completion of this project. I am also very thankful to the Chief editor, Punjab University Journal of Mathematics that he has given me a chance to improve my article up to the standard and able to publish.

REFERENCES

- [1] A. Asheim, *Applying the numerical method of steepest descent on multivariate oscillatory integrals in scattering theory*, arXiv preprint arXiv:1302.1019 (2013).
- [2] A. Asheim and D. Huybrechs, *Asymptotic analysis of numerical steepest descent with path approximations*, *Found. Comput. Math.* **10**, (2010) 647–671.
- [3] S. I. Aziz and W. Khan, *Quadrature rules for numerical integration based on Haar wavelets and hybrid functions*, *Comp. Math. Appl.* **61**, (2011) 2770–2781.
- [4] A. Deano and D. Huybrechs, *Complex Gaussian quadrature of oscillatory integrals*, *Numer. Math.* **112**, No. 2 (2009) 197–219.
- [5] G. A. Evans and K. C. Chung, *Some theoretical aspects of generalized quadrature methods*, *J. Complexity* **19**, No. 3 (2003) 272–285.
- [6] G. A. Evans and J. R. Webster, *A comparison of some methods for the evaluation of highly oscillatory integrals*, *J. Comput. Appl. Math.* **112**, (1999) 55–69.
- [7] L. N. G. Filon, *On a quadrature formula for trigonometric integrals*, *Proc. Roy. Soc. Edinburgh* **49**, (1928) 38–47.

- [8] L. N. G. Filon, *On a quadrature formula for trigonometric integrals*, Proc. Roy. Soc. **49**, (2005) 38–47.
- [9] D. Huybrechs and S. Olver, *Superinterpolation in highly oscillatory quadrature*, Found. Compt. Math. **12**, (2012) 203–228.
- [10] D. Huybrechs and S. Vandewalle, *On the evaluation of highly oscillatory integrals by analytic continuation*, SIAM J. Numer. Anal. **44**, No. 3 (2006) 1026–1048.
- [11] A. Iserles, *On the numerical quadrature of highly-oscillatory integrals ii: Irregular oscillators*, IMA J. Numer. Anal. **25**, (2005) 25–44.
- [12] A. Iserles and S. P. Norsett, *On quadrature methods for highly oscillatory integrals and their implementation*, BIT Numer. Math. **44**, No. 4 (2004) 755–772.
- [13] A. Iserles and S. P. Norsett, *Efficient quadrature of highly oscillatory integrals*, Proc. Roy. Soc. **461**, (2005) 1383–1399.
- [14] A. Iserles and S. P. Norsett, *On the computation of highly oscillatory multivariate integrals with stationary points*, BIT, Numer. Math. **46**, No. 3 (2006) 549–566.
- [15] A. Iserles and S. P. Norsett, *On quadrature methods for highly oscillatory integrals and their implementation*, BIT Num. Math. **44**, (2004) 755–772.
- [16] A. Iserles, *Wave propagation and scattering in random media*, Academic press New York, **2**, (1978).
- [17] S. U. Islam, A. A. S. Fhaid and S. Zaman, *Meshless and wavelet based complex quadrature of highly oscillatory integrals and the integrals with stationary points*, Eng. Anal. Bound. Elemt. **37**, (2013) 1136–1144.
- [18] S. U. Islam, I. Aziz and F. Haq, *A comparative study of numerical integration based on Haar wavelets and hybrid functions*, Comp. Math. Appl. **59**, (2010) 2026–2036.
- [19] S. U. Islam, I. Aziz and W. Khan, *Numerical integration of multi-dimensional highly oscillatory, gentle oscillatory and non-oscillatory integrands based on wavelets and radial basis functions*, Eng. Anal. Bound. Elemt. **36**, (2012) 1284–1295.
- [20] S. U. Islam and S. Zaman, *New quadrature rules for highly oscillatory integrals with stationary points*, J. Comp. Appl. Math. **278**, (2015) 75–89.
- [21] J. Li, T. W. X. Wang and S. Xiao, *An improved Levin quadrature method for highly oscillatory integrals*, J. Appl. Numer. Math. **60**, (2010) 833–842.
- [22] Y. Liu, *Fast evaluation of canonical oscillatory integrals*, Appl. Math. **6**, No. 2 (2012) 245–251.
- [23] D. Levin, *Procedures for computing one and two-dimensional integrals of functions with rapid irregular oscillations*, Math. Comp. **158**, (1982) 531–538.
- [24] S. Olver, *Moment-free numerical approximation of highly oscillatory integrals with stationary points*, Eur. J. Appl. Math. **18**, (2007) 435–447.
- [25] S. Olver, *Fast and numerically stable computation of oscillatory integrals with stationary points*, BIT **50**, (2010) 149–171.
- [26] K. Shariff and A. Wray, *Analysis of the radar reflectivity of aircraft vortex wakes*, J. Fluid. Mech. (2002).
- [27] S. Xiang, *Efficient Filon-type methods for $\int_a^b f(x)e^{i\omega g(x)} dx$* , Numer. Math. **105**, (2007) 633–658.
- [28] S. Xiang, *Efficient quadrature for highly oscillatory integrals involving critical points*, J. Comp. Appl. Math. **206**, (2007) 688–698.
- [29] S. Xiang and W. Gui, *On generalized quadrature rules for fast oscillatory integrals*, Appl. Math. Comput. **197**, No. 1 (2008) 60–75.
- [30] S. Xiang and H. Wang, *Fast integration of highly oscillatory integrals with exotic oscillators*, Math. Comput. **79**, No. 270 (2010) 829–844.
- [31] S. Zaman and S. U. Islam, *Efficient numerical methods for Bessel type of oscillatory integrals*, J. Comp. Appl. Math. **315**, (2017) 161–174.